Molecular Biology of the Cell
Vol. 11, 2069–2083, June 2000

Histone Deacetylase Inhibitors Trigger a G2 Checkpoint in Normal Cells That Is Defective in Tumor Cells

Ling Qiu,*† Andrew Burgess,*† David P. Fairlie,‡ Helen Leonard,* Peter G. Parsons,* and Brian G. Gabrielli*§

*Queensland Cancer Fund Laboratories, Queensland Institute of Medical Research, and Joint Experimental Oncology Program, Department of Pathology, University of Queensland, Brisbane, Queensland, Australia; and ‡Centre for Drug Design and Development, University of Queensland, St. Lucia, Queensland, Australia

Submitted December 27, 1999; Revised March 17, 2000; Accepted March 29, 2000
Monitoring Editor: Alan P. Wolffe

Important aspects of cell cycle regulation are the checkpoints, which respond to a variety of cellular stresses to inhibit cell cycle progression and act as protective mechanisms to ensure genomic integrity. An increasing number of tumor suppressors are being demonstrated to have roles in checkpoint mechanisms, implying that checkpoint dysfunction is likely to be a common feature of cancers. Here we report that histone deacetylase inhibitors, in particular azelaic bishydroxamic acid, triggers a G2 phase cell cycle checkpoint response in normal human cells, and this checkpoint is defective in a range of tumor cell lines. Loss of this G2 checkpoint results in the tumor cells undergoing an aberrant mitosis resulting in fractured multinuclei and micronuclei and eventually cell death. This histone deacetylase inhibitor-sensitive checkpoint appears to be distinct from G2/M checkpoints activated by genotoxins and microtubule poisons and may be the human homologue of a yeast G2 checkpoint, which responds to aberrant histone acetylation states. Azelaic bishydroxamic acid may represent a new class of anticancer drugs with selective toxicity based on its ability to target a dysfunctional checkpoint mechanism in tumor cells.

INTRODUCTION

A complex series of controls ensure ordered progression through the cell cycle. Incomplete replication, the presence of unrepaired DNA, or incorrect spindle assembly initiates an arrest of cell cycle progression through a checkpoint mechanism (Elledge, 1996). Checkpoints ensure that progression through key cell cycle phase transitions occurs only after successful and accurate completion of the preceding phase. Failures in these checkpoints can lead to the transmission of a mutated genome, the consequence of either incomplete replication, genetic mutations, or the loss or gain of chromosomes, to future generations. These genetic aberrations may result in the loss of a growth suppressor or acquisition of a growth promotor and usually accompany further genomic instability, a hallmark of cancer (Hartwell and Kastan, 1994; Lengauer *et al.*, 1997). A number of genes identified as tumor suppressors have important roles in checkpoints, e.g., p53, Rb, and BRCA1, and loss or mutation of tumor suppressor genes is a common feature in the development of many types of cancer (Elledge, 1996; Sherr, 1996).

The primary components of the cell cycle machinery are cyclin-dependent kinases (cdks). This family of related serine-threonine kinases are regulated by association with regulatory cyclin subunits and a series of phosphorylations and dephosphorylations (Morgan, 1995). A further level of cdk regulation is via the cyclin-dependent kinase inhibitor proteins, which directly bind the cdks. Two families of these proteins have been identified, the $p21^{Waf1/Cip1}$ and $p16^{INK4/CDKN2A}$ families (Sherr and Roberts, 1995). The cdk/cyclins are the ultimate targets of the checkpoint pathways. This is best illustrated by the ionizing radiation–induced G1 checkpoint, which is mediated by the tumor suppressor gene product p53, which increases the expression of p21, in turn inhibiting cdk2/cyclin activity necessary for progression from G1 into S phase (Dulic *et al.*, 1994; Wang, 1998). There are also DNA damage checkpoints in G2, which are imposed through a block in the cdc25-dependent activation of the mitotic cdk/cyclins (Gabrielli *et al.*, 1997; Wang, 1998), and an anaphase checkpoint that senses

† These authors contributed equally to this work.
§ Corresponding author: Department of Pathology, University of Queensland Medical School, Herston, Queensland 4006, Australia. E-mail address: briang@mailbox.uq.edu.au.

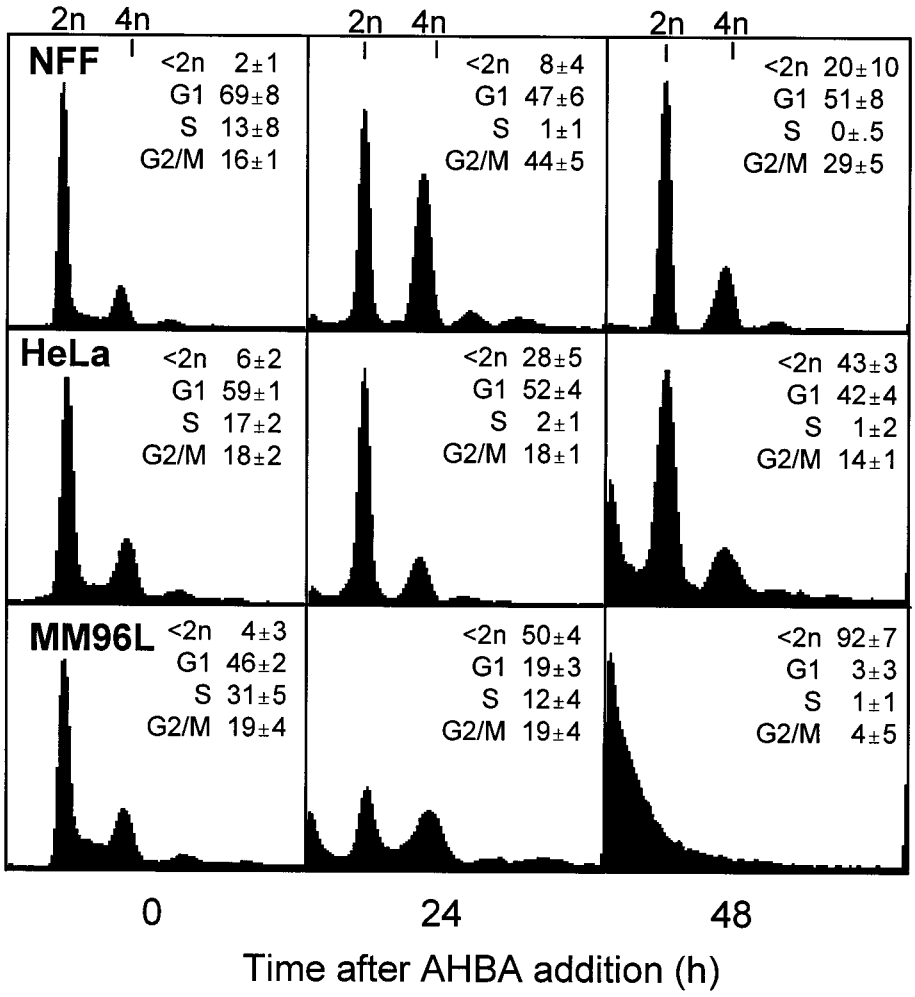

Figure 1. ABHA induces a G2/M arrest in resistant cells. Cultures of ABHA-resistant NFF and ABHA-sensitive HeLa and MM96L cells were treated with 100 μg/ml ABHA for the indicated times and then harvested and analyzed by FACS for their cell cycle status. The percentage of subdiploid (<2n), G1, S, and G2/M phase cells are reported as mean ± SD from three to five separate experiments.

the correct assembly of the condensed chromosomes onto the mitotic spindle and bipolar microtubule attachment of the kinetochores (Sorger *et al.*, 1997). Failure to do so results in the cells arresting in mitosis rather than transiting into the subsequent G1.

Loss of cell cycle checkpoints provides a growth advantage for tumor cells, but paradoxically, it is also loss of a protective mechanism. Thus cells with dysfunctional checkpoints are also more sensitive to agents that would normally trigger a response from the defective checkpoint. For example, cells carrying a mutation in the *ATM* gene, which is involved in checkpoint response to DNA damage induced by genotoxins such as ionizing radiation, are more susceptible to killing by these agents (Lavin and Shiloh, 1996). Thus the identification of checkpoint genes, defining their normal functions and the cellular stresses to which they respond, has important implications for the development of new anticancer treatments.

The anticancer potential of histone deacetylase inhibitors has been widely acknowledged (Saito *et al.*, 1999; Saunders *et al.*, 1999). These compounds block histone deacetylase activity, resulting in a profound increase in the acetylation state of the chromatin, which in turn affects chromatin structure and regulation of gene expression (Grunstein, 1997). Histone deacetylase inhibitors block cell proliferation by up-regulating the expression of the cdk inhibitor $p21^{Cip1/Waf1}$, inducing a G1 phase arrest and a differentiated phenotype in a range of tumor cell types (Sowa *et al.*, 1997; Archer *et al.*, 1998; Richon *et al.*, 1998; Saito *et al.*, 1999; Saunders *et al.*, 1999). The histone deacetylase inhibitor azelaic bishydroxamic acid (ABHA) has been demonstrated to selectively and permanently arrest the growth of a range of tumor and transformed cell lines, without affecting normal cell lines (Parsons *et al.*, 1997; Qiu *et al.*, 1999). ABHA is also a potent differentiation-inducing factor (Breslow *et al.*, 1991), although in melanoma cell lines the only indication of differentiation is a more dendritic morphology, other differentiation markers being unaffected (Parsons *et al.*, 1997). The molecular basis of this selective toxicity is not attributable to differential sensitivity of histone deacetylases in these cell lines to inhibition by ABHA, because the levels of histone acetylation observed after ABHA treatment were similar in sensitive and resistant cell lines (Qiu *et al.*, 1999). In this report we have investigated the basis of the selectivity of ABHA and uncovered a novel G2 checkpoint activated by histone deacetylase inhibitors in resistant cells, which is

defective in sensitive cells. The loss of this checkpoint appears to be a major determinant of the sensitivity to this class of drugs, and the apparently widespread loss of this checkpoint may account for the tumor cell selectivity of ABHA.

MATERIALS AND METHODS

Materials

Trichostatin A (TSA), sodium butyrate, hexamethylene bisacetamide (HMBA), etoposide, and nocodazole were purchased from Sigma (St. Louis, MO). ABHA and azelaic-1-hydroxamate-9-anilide (AAHA) were generously synthesized by Mike West (Center for Drug Design and Development, University of Queensland). The topoisomerase II inhibitor ICRF193 was a generous gift from Dr. A.M. Creighton (St. Bartholemew's Hospital, London, United Kingdom). All chemicals used were analytical grade.

Cell Lines and Culture Conditions

The human cervical cancer cell line HeLa, human melanoma cell lines MM96L, SK-Mel-13, A2058, and MM229, and primary cultures of neonatal foreskin fibroblasts (NFFs) were cultured in RPMI-1640 medium containing 5 or 10% (vol/vol) fetal calf serum. Assays for *Mycoplasma* were carried out monthly to ensure that the cultured cells were free of contamination. Asynchronous cultures of each cell line were treated with 100 μg/ml ABHA, 100 ng/ml TSA, 10 μg/ml AAHA, 5 mM sodium butyrate, or HMBA for 24 h and then harvested for immunoblotting, immunoprecipitation, or flow cytometric analysis. In some cases, cultures were treated with 0.5 μg/ml ICRF193, 600 nM etoposide, or 0.5 μg/ml nocodazole for 24 h to produce G2 or M phase–arrested populations.

3-[4,5-Dimthylthiazol-2yl]-2,5-Diphenyltetrazolium Bromide (MTT) Cell Proliferation Assay

Cells in log phase growth were seeded into 96-well plates at a density of 2–5 $\times$ 10^3 on the day before addition of 100 μg/ml ABHA. Cell proliferation was measured using MTT, which measures mitochondrial activity of viable cells. MTT was added to the culture media at a final concentration of 0.5 mg/ml, and the plates were incubated for 4 h at 37°C. The insoluble Formazan product was then precipitated by centrifuging the plates, the supernatant was removed, and the Formazan crystals were dissolved in 100 μl of DMSO with gentle shaking at room temperature. Absorbance at 570 nm was measured using a Bio-Rad (Hercules, CA) microplate reader.

Cell Synchrony and Flow Cytometry

Cells were synchronized in late G1/early S phase by addition of 2 mM hydroxyurea for 24 h and then released from this block by washing and addition of fresh media. ABHA or TSA was added 2 h after release from the hydroxyurea block as the cells were progressing through early S phase. Control untreated or treated cells were harvested at 8, 12, 24, and 48 h after release from the hydroxyurea block for either flow cytometry or biochemical analysis. Both attached and floating cells were collected. For flow cytometric analysis, cells were fixed in 70% ethanol at 0°C, and the nuclear DNA was stained using a solution of propidium iodide (50 μg/ml), RNase A (1 mg/ml), and Triton X-100 (0.02%) in PBS. The stained cells were filtered through fine gauze, and the single-cell suspensions were analyzed on a FACScalibur (Becton Dickinson, Franklin Lakes, NJ) using CellQuest and ModFit data analysis software.

Asynchronous cultures were labeled with 10 μM bromodeoxyuridine (BrdU) for 2 h, treated with 100 μg/ml ABHA for 24 h, and then harvested and fixed with 70% ethanol at −20°C. The fixed cells were suspended in 2 M HCl and 0.5% (vol./vol) Triton X-100 for 30 min at room temperature. The cells were neutralized by resuspending them in 0.1 M Na tetraborate, pH 8.5, for 5 min at room temperature. BrdU incorporation was detected by staining with FITC-conjugated anti-BrdU monoclonal antibody (Becton Dickson), the DNA was counterstained with propidium iodide, and cells were analyzed by two-dimensional flow cytometry.

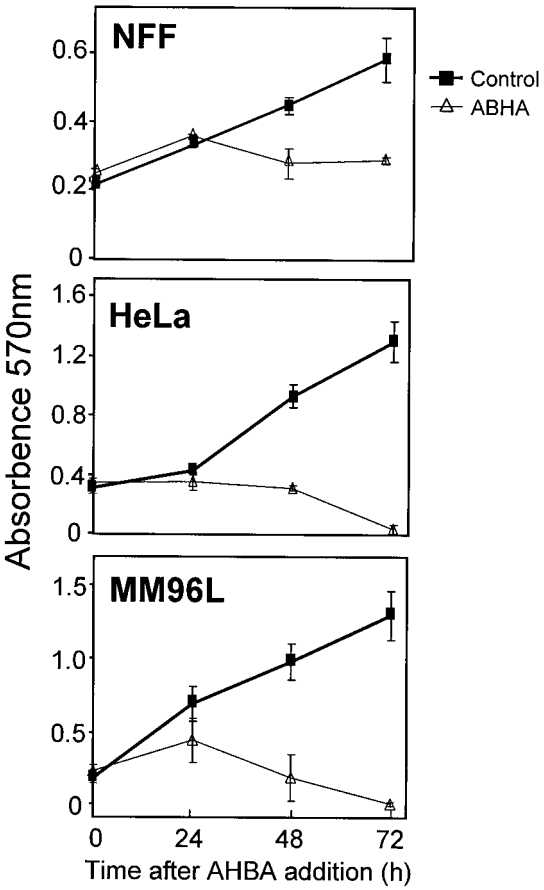

Figure 2. ABHA induces proliferative arrest and cell death. MTT assays were performed on the indicated cell lines over 72 h with or without addition of 100 μg/ml ABHA. The data are the mean ± SD of triplicate determinations.

Immunoblotting

Cell pellets were dispersed by sonication in 300 μl of cell lysis buffer (20% glycerol, 1% SDS, 10 mM Tris, pH 7.4, and 2 mM PMSF), boiled for 5 min, and then centrifuged at 15,000 rpm for 15 min to obtain a clarified soluble fraction. Samples were stored at −70°C until use. Protein quantitation was performed using bicinchoninic acid (Pierce, Rockford, IL) using γ-globulin as a standard. Samples were resolved on 12% SDS-PAGE and then transferred to nitrocellulose membranes. The levels of various cell cycle regulatory proteins were detected using antibodies against Rb and cyclin A (PharMingen, San Diego, CA), cyclin B1 and cdc25C (Gabrielli *et al.*, 1996), cdc2 and cdk2 (Santa Cruz Biotechnologies, Santa Cruz, CA), $p21^{Cip1/Waf1}$ (Calbiochem, La Jolla, CA), and $p27^{Kip1}$ (Transduction Laboratories, Lexington, KY), detected with the appropriate horseradish peroxidase-conjugated secondary antibody using enhanced chemiluminescent (New England Nuclear, Boston, MA) detection. Equal amounts of protein (20 μg of protein) were loaded, confirmed in some experiments by Coomassie blue staining of a gel run in parallel.

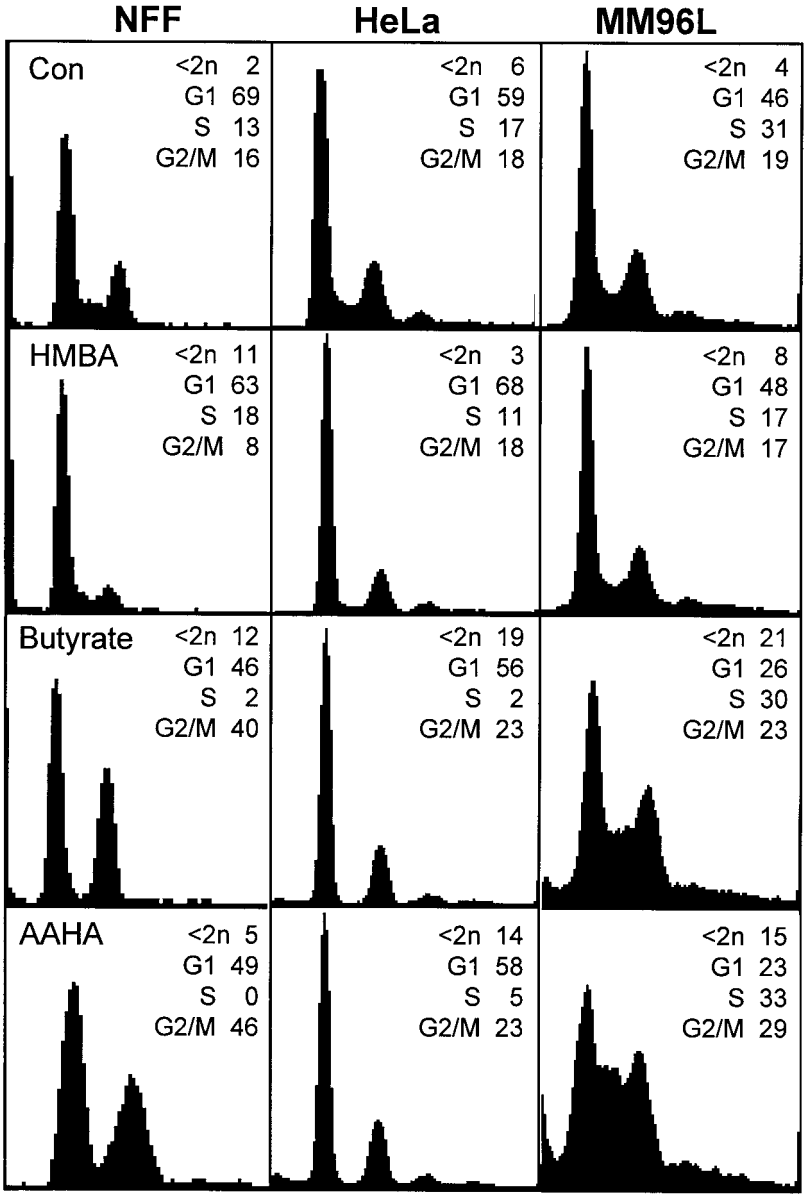

Figure 3. Treatment with a range of histone deacetylase inhibitors produces similar cell cycle effects. Cultures of the indicated cell lines, either asynchronously growing controls (Con) or treated with 5 mM HMBA, 5 mM sodium butyrate, or 10 μg/ml AAHA and then harvested after 24 h, were analyzed by FACS for their cell cycle status as in Figure 1. These data are representative of three separate experiments.

Immunoprecipitation and cdk Kinase Assay

Cells (1–5 $\times$ 10^6) were lysed in NETN buffer (20 mM Tris, pH 8.0, 100 mM NaCl, 1 mM EDTA, and 0.5% Nonidet P-40) supplemented with 0.3 M NaCl, 5 μg/ml leupeptin, apoprotin, and pepstatin, 0.5 mM PMSF, 10 mM NaF, and 0.1 mM sodium vanadate. The cleared lysates were incubated with anti-cdk2 and anti-cyclin B1 (1–2 μg of antibody) antibodies prebound to 30 μl of 50% suspension of protein A-Sepharose for 3 h at 4°C. The precipitates were washed four times with NETN and assayed for histone H1 kinase activity as described previously (Gabrielli *et al.*, 1997). The histone phosphorylation was quantitated by PhosphorImager (Molecular Dynamics, Sunnyvale, CA).

Immunofluorescent Staining

Cells were grown on glass coverslips. For immunostaining, cells were washed with PBS and then fixed with −20°C methanol and stored at −20°C until required. Coverslips were fixed to a glass microscope slide, allowed to air dry, and then rehydrated with PBS containing 0.1% Tween 20 and 3% BSA for 1 h at room temperature. The cells were stained with anti-α-tubulin (1:1000 dilution; Amersham, Arlington Heights, IL) and human autoimmune serum to detect kinetochores (1:500 ACA serum; a gift from Dr. J.B. Rattner, University of Calgary, Calgary, Alberta, Canada) and DAPI for DNA. Photomicroscopy was performed as described previously (Gabrielli *et al.*, 1996).

RESULTS

Histone Deacetylase Inhibitors Impose G1 and G2/M Phase Cell Cycle Arrest

We have examined a number of cultured cell types with varying sensitivity to killing by ABHA: ABHA-resistant NFF

cultures (D_{37} >300 μg/ml) and MM229 (D_{37} 180 μg/ml), ABHA-sensitive HeLa, A2058, and SK-Mel-13 cell lines (D_{37} <50 μg/ml), and hypersensitive MM96L (D_{37} 10 μg/ml) (Parsons *et al.*, 1997). Only data from experiments with a representative cell line from each sensitivity group, NFF, HeLa, and MM96L, are shown, although essentially identical results were obtained with the other cell lines in each group.

A difference was observed in the cell cycle distributions of ABHA-sensitive tumor cells and ABHA-resistant cultures after treatment with a dose (100 μg/ml) of ABHA that was toxic to the tumor cells lines, whereas NFF cells were resistant to killing at this concentration (Parsons *et al.*, 1997). NFF cultures showed an increased G2/M population at 24 and 48 h and an emptying of the S phase compartment (Figure 1). These cell cycle changes are indicative of arrests in G1 and G2/M phases of the cell cycle. Loss of S phase cells was also observed in ABHA-treated HeLa cultures, but there was no evidence of a G2/M phase accumulation, suggesting only a G1 phase arrest. By contrast, ABHA reduced the proportion of G1 phase cells in cultures of MM96L at 24 h, and there was a significant increase in the proportion of subdiploid cells (<2n DNA content), likely to be dying cells (Darzynkiewicz *et al.*, 1992), although the persistence of an S phase population suggests that some proportion of these cultures were still actively cycling. By 48 h, >90% of MM96L cells had <2n DNA content, and >40% HeLa cells were subdiploid, whereas only 20% of the NFF cells were subdiploid at this time (Figure 1). [^{3}H]Thymidine incorporation studies confirmed the loss of S phase cells in ABHA-treated NFF and HeLa cultures at 24 h after treatment. ABHA treatment also reduced the levels of [^{3}H]thymidine incorporation in MM96L cells to 30% of controls, indicating that a reduced proportion of cells were in S phase, supporting the fluorescence-activated cell sorting (FACS) data (our unpublished results).

To confirm that the increase in the subdiploid population observed in the ABHA-treated tumor cells was due to dying cells, MTT proliferation assays were performed. NFF cultures cycled normally until 24 h after treatment and then arrested, whereas MM96L cultures had reduced proliferation, and HeLa cells were completely blocked at this time (Figure 2). For both HeLa and MM96L cultures, the viable population decreased at 48 h after treatment to levels below those at the start of the experiment, and by 72 h there was complete loss of viability in the tumor cell lines (Figure 2). The reduction in the numbers of viable cells in the tumor cell cultures correlated with the increased proportion of subdiploid cells observed by FACS (Figure 1).

Other histone deacetylase inhibitors, sodium butyrate and the ABHA derivative AAHA, were also found to have a similar spectrum of cell cycle effects as ABHA in both normal and tumor cell cultures. The related compound HMBA, which does not inhibit histone deacetylase activity (Richon *et al.*, 1998), only partly reduced the S phase population and did not produce a G2/M arrest in NFF cultures but actually reduced the proportion of G2/M phase cells (Figure 3).

The changes in cell cycle distribution detected by flow cytometry suggested that ABHA treatment imposed a G1 phase arrest in NFF and HeLa cells but not MM96L cells. This was confirmed by analysis of the G1/S regulators Rb and cyclin A/cdk2. Immunoblotting of lysates from equal numbers of either untreated control or ABHA-treated cells at 24 h after treatment revealed no changes in Rb protein levels but a loss of the hyperphosphorylated forms of Rb in ABHA-treated HeLa and NFF cells, detected by the reduction from multiple to a single, tight electrophoretic species, consistent with the G1 arrest observed in NFF and HeLa cells (Figure 1). No change in Rb was noted in MM96L cells, which do not arrest in G1 (Figure 3). No changes were observed in the levels of cdk2, but its partner cyclin A was down-regulated in HeLa and NFF cells. The cdk inhibitor p21 was increased in both HeLa and NFF cells but not in MM96L cells (Figure 4A), and no effect on the levels of two other cdk inhibitors, p16 and p27, was observed (our unpublished results).

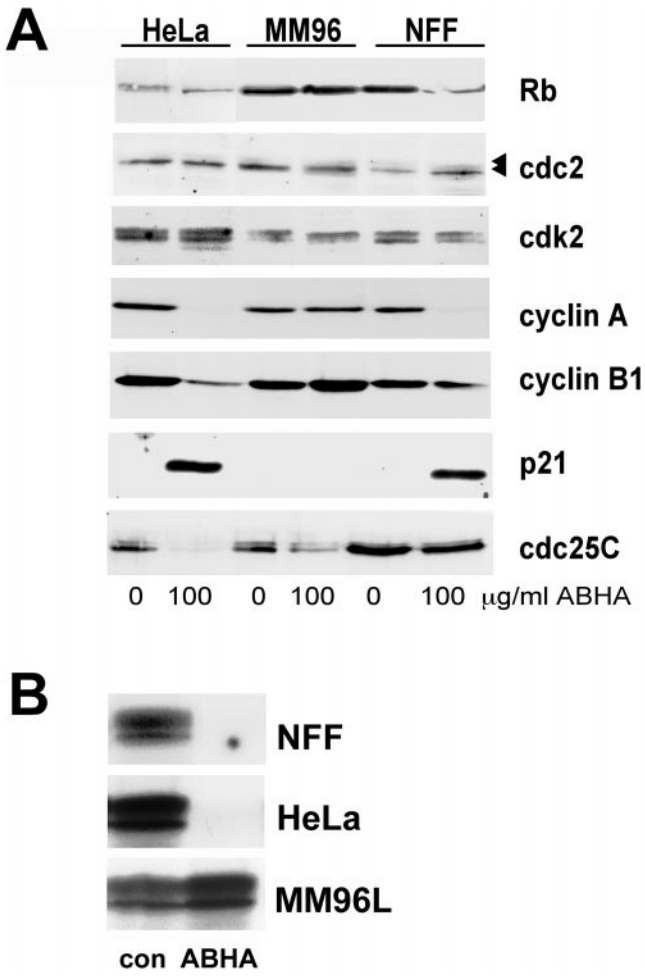

Figure 4. ABHA treatment affects the expression and activity of cell cycle regulators. (A) Cells were treated with 100 μg/ml ABHA as indicated and harvested after 24 h, lysed, and immunoblotted for the indicated cell cycle regulatory proteins. The positions of the hyper- and hypophosphorylated forms of Rb and cdc2 are indicated by the arrowheads. (B) Cdk2 immunoprecipitate H1 kinase activity was assessed from cells treated as in A. No phosphorylation of H1 was detected in the ABHA-treated NFF sample even on longer exposures.

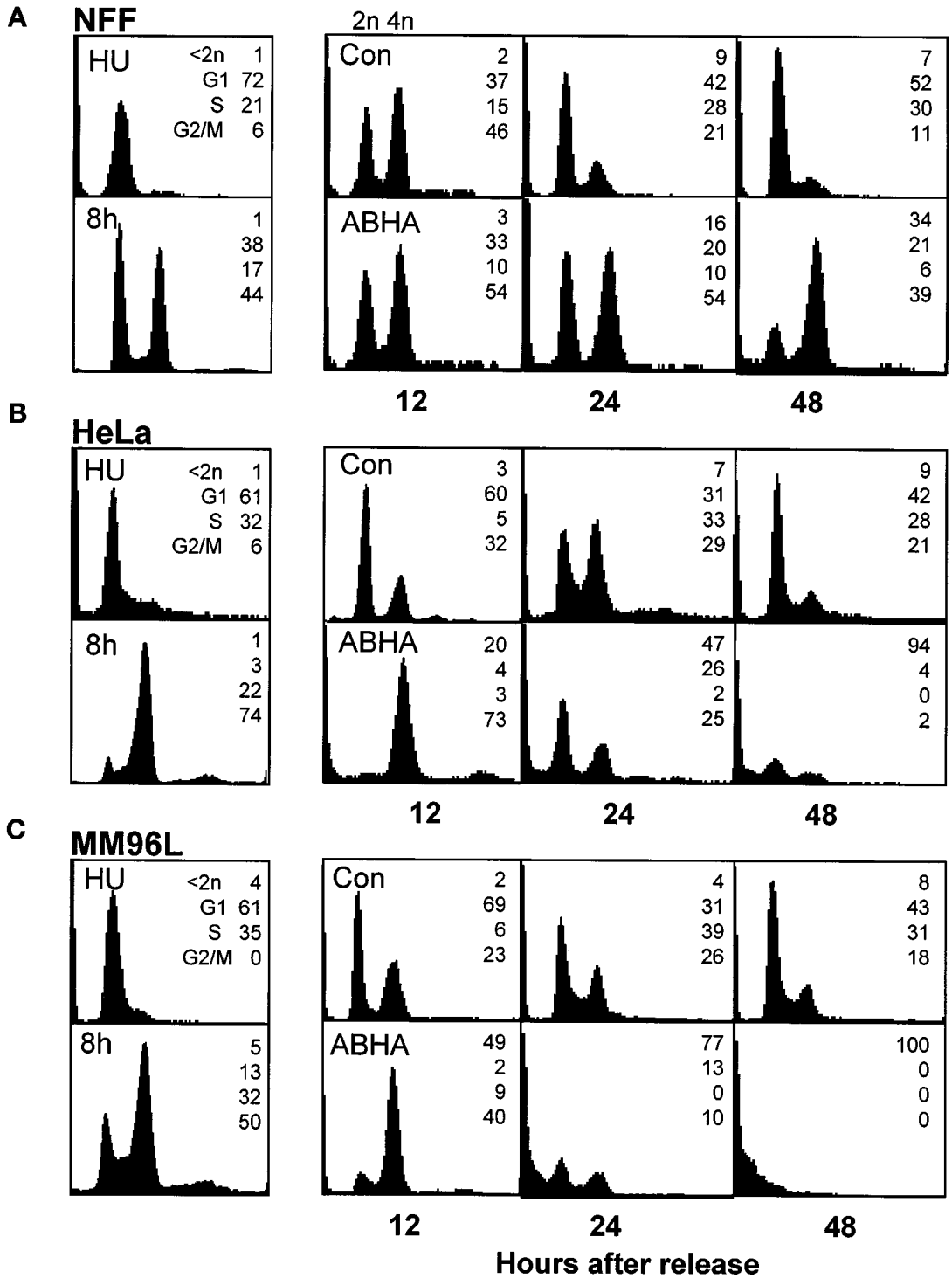

Figure 5.

The activity of the cdk2/cyclin A complexes, which have functions in S and G2/M phases of the cell cycle (Dulic *et al.*, 1992; Rosenblatt *et al.*, 1992; Pagano *et al.*, 1993), reflected the increased p21 and decreased cyclin A levels. The cdk2 activity was undetectable in NFF cultures and strongly suppressed in HeLa cells (5% of control levels) after ABHA treatment, whereas the ABHA-treated MM96L cells had similar activity to the controls (Figure 4B). Taken together, these

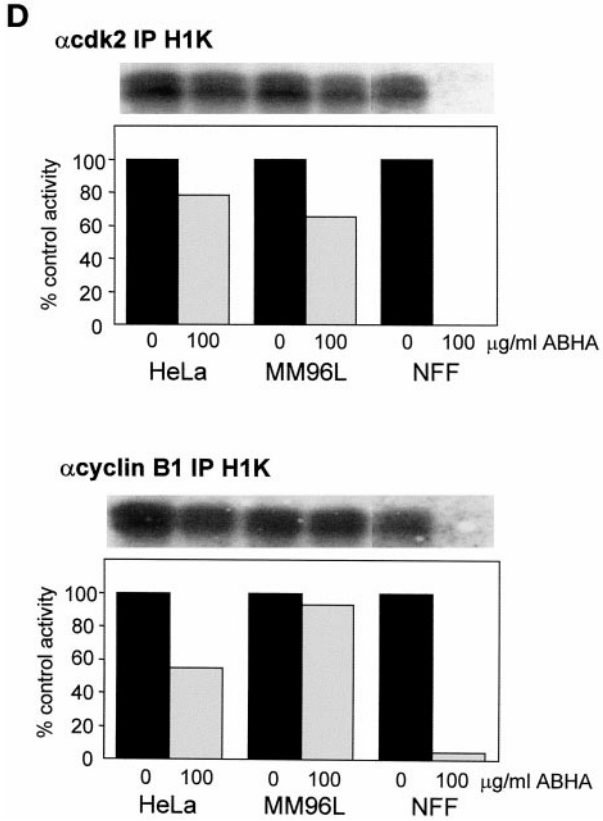

Figure 5 (facing page). Sensitive but not resistant cells transit through mitosis in the presence of ABHA. (A–C) Cells were synchronized at G1/S by overnight treatment with hydroxyurea (HU) and then released from the arrest and treated without (Con) or with 100 μg/ml ABHA (ABHA) 2 h after release. Cells were harvested at the indicated times after release and analyzed by FACS for their cell cycle status as in Figure 1. The 8-h control time point is shown as a measure of the synchrony obtained. The data presented are representative of three to five separate experiments. Identical data were obtained using 100 ng/ml TSA in place of ABHA (our unpublished results). (D) The activity of cyclin A/cdk2 and cyclin B1/cdc2 was assessed by anti-cdk2 and anti-cyclin B1 immunoprecipitate kinase assays from samples of the indicated cell lines harvested at 12 h after release from a hydroxyurea block and treated without or with 100 μg/ml ABHA as in A–C. The autoradiogram of the phosphorylated histone H1 and activity expressed as percentage of the control for each cell line are shown.

data support the cell cycle arrests in both NFF and HeLa cell cultures observed by FACS at 24 h after treatment with ABHA and the lack of arrest in MM96L cultures (Figure 1).

The levels of G2/M regulatory proteins revealed little effect on either the levels or phosphorylation status of cdc2 as detected by electrophoretic mobility shift (Figure 4A) or immunoblotting with a cdc2 and cdk2 phosphotyrosine 15-specific antibody (our unpublished results). The level of cyclin B1 was reduced in HeLa cells (Figure 4A). Interestingly, the level of cdc25C, one of the activators of cdc2/cyclin B in mitosis, was greatly reduced in both HeLa and MM96L cells but unaffected in NFF cells. The loss of cdc25C expression in both tumor cell lines suggests that these cells would be incapable of reentering a second round of mitosis after 24 h ABHA treatment.

Absence of a G2 Arrest Correlates with Increased Sensitivity to ABHA

The accumulation of cells with 4n DNA content in the ABHA-treated NFF cultures suggested that these cells were arrested in G2/M, and the lack of this accumulation in the tumor cells may be due to either the lack of a G2/M arrest or cells dying before reaching G2/M. Cultures were synchronized using a hydroxyurea block release to examine whether cells were capable of transiting through G2/M in the presence of ABHA. In each case, the untreated control cells transited through S into G2 phase by 8 h with >60% synchrony (NFFs were the exception, with up to 50% of cells failing to exit the G1 arrest; see the 8-h time point in Figure 5A), reached mitosis by 10–12 h after release, and had returned to asynchronous cycling by 24–48 h after release (Figure 5, A–C). The ABHA-treated NFF cultures appeared blocked in G1 and G2/M at 24 h, with the G1 cells likely to be those that did not recommence cycling after the hydroxyurea block (Figure 5A). ABHA treatment of both tumor cell lines slowed their progression through G2/M, demonstrated by the greater accumulation of 4n cells compared with the controls at 12 h after release (Figure 5, B and C). The cells did, however, progress through mitosis, demonstrated by the reduction in the 4n population at 24 h. The cell cycle effects produced by ABHA were due to its histone deacetylase inhibitor activity, because substitution with 100 ng/ml trichostatin A produced essentially identical results (our unpublished results).

A striking consequence of ABHA treatment of the synchronized tumor cells was the increase in the proportion of subdiploid cells detected at 24 and 48 h after release from the hydroxyurea block. In HeLa and MM96L cultures there was an approximately twofold increase in the proportion of subdiploid cells detected at 24 h after release compared with 24 h after treatment of asynchronous cultures (increased from 28 to 47% in HeLa and 50 to 77% in MM96L for asynchronous and synchronous treatment, respectively; Figures 1 and 5). At 48 h after release, ABHA treatment resulted in up to 100% subdiploid cells in both cell lines. ABHA treatment of unsynchronized HeLa cultures resulted in only 75% cells with <2n DNA content after 72 h. A similar, although smaller, effect was observed with synchronized NFF cultures, with <35% subdiploid cells compared with 100% in the tumor cell cultures at 48 h, and appeared to correlate with the decrease in G1 phase cells (Figure 5A). The increased subdiploid population did not appear to be a consequence of some inherent toxicity of hydroxyurea treatment, because in some experiments a thymidine block release protocol was used to synchronize HeLa cell cultures in place of hydroxyurea, and ABHA treatment produced a similar increase in cell death at 24 and 48 h.

As a further measure of cell cycle progression through mitosis, the activity of the mitotic cyclin/cdk activities, cyclin A/cdk2 and cyclin B1/cdc2, was assayed from the synchronized cultures at 12 h after release. The mitotic cyclin/cdk activity in the ABHA-treated tumor cell samples was >60% of the control levels, whereas little or no activity was detected in the ABHA-treated NFF cultures (Figure 5D). FACS analysis indicated that the tumor cell lines were re-

tarded through G2/M, and visual inspection of cultures for the rounded mitotic phenotype confirmed that ABHA treatment delayed entry into mitosis by 1–2 h in the tumor cell lines. This slowdown in G2/M progression is likely to account for the reduced cyclin/cdk activity in the ABHA-treated tumor cells. The complete absence of both cyclin A/cdk2 activity, which is activated in early G2 phase, and cyclin B1/cdc2, which is activated at the G2/M transition, and the absence mitotic cells in ABHA-treated NFF cultures confirmed the G2 arrest in NFF cells observed by FACS (Figure 5A).

Progression of the ABHA-treated HeLa cells, but not NFF cells, through G2/M was also observed by following BrdU-labeled S phase cells from asynchronously growing cultures. Control cultures of NFF and HeLa cells displayed normal progression through S into G2/M phase by 6 h and progressed into G1 and S phase again by 24 h after BrdU labeling (Figure 6, A and B, Con). In ABHA-treated NFF cultures, BrdU-labeled cells accumulated in the 4n peak at 6 h and remained blocked there at 24 h, whereas a large proportion of the 4n population in ABHA-treated HeLa cultures detected at 6 h had returned to the 2n peak by 24 h, indicating that these cells have undergone mitosis and cytokinesis (Figure 6B).

Lack of ABHA-sensitive G2 Arrest Leads to Aberrant Mitosis

These data correlated the absence of an ABHA-induced G2/M arrest in the tumor cell lines with increased sensitivity to killing by histone deacetylase inhibitors and the G2 arrest in NFF cells with protection from the cytotoxic effects of ABHA. This is reminiscent of the loss of a cell cycle checkpoint. Loss of the G2/M checkpoint is associated with cells undergoing some form of aberrant mitosis and resultant daughter cells containing fractured DNA often seen as micronuclei and eventually cell death (Jin *et al.*, 1996; Rhind *et al.*, 1997). To examine whether the absence of a G2/M arrest in the ABHA-treated tumor cells produced a similar aberrant mitotic phenotype, hydroxyurea synchronized cells, both control and ABHA treated, were fixed when rounded mitotic cells were observed, 12–14 h after release from the hydroxyurea block. The cells were stained for microtubules, kinetochores, and DNA and inspected by fluorescence microscopy (Figure 7). In the control cultures, metaphase and anaphase figures we observed, showing normal chromosome condensation and migration to the metaphase plate, and undergoing anaphase–telophase separation of sister chromatids (Figure 7, a–c). Staining for kinetochores showed the metaphase and anaphase movement of chromosomes very clearly (Figure 7b). In the ABHA-treated cells, chromosome condensation and mitotic spindle formation appeared to be relatively normal (Figure 7, d and f). However, few cells were observed with a properly formed metaphase plate, and most appeared to have some defect in chromosomal congression, and it was common to see cells with chromosomes surrounding the spindle poles and kinetochores on the astral side of the spindle pole (Figure 7, e and f). A similar noncongression phenotype was found in ABHA-treated asynchronous cultures and in two other melanoma cell lines, SK-Mel-13 and A2058. Quantitation of the noncongression phenotype in HeLa and MM96L cultures revealed that >80% of the mitotic cells in the ABHA-treated cultures displayed this form of aberrant mitosis (Figure 7G). No mitotic figures were found in ABHA-treated NFF cultures, and all had an interphase appearance.

The consequence of noncongression was cells undergoing mitosis without proper partitioning of the replicated chromosomes, resulting in cells containing multiple nuclei and mini nuclei (Figure 8, b, c, and f, *m*), and in some cases the cells had attempted to undergo cytokinesis with incompletely separated chromosomes resulting in the classical "cut" phenotype (Figure 8e, *c*), characteristic of a loss of G2/M checkpoint arrest in yeast (Rhind *et al.*, 1997). There was also evidence of apoptosis, with cells displaying multiple, brightly stained micronuclei characteristic of apoptosis (Figure 8 e and f, *a*).

ABHA Triggers a Novel G2 Checkpoint

The absence of a G2 arrest and the consequent aberrant mitotic phenotype and increased sensitivity to killing by ABHA in the tumor cell lines indicated that a G2 checkpoint mechanism responsive to histone deacetylase inhibitors was defective in these cell lines. To establish whether this was one of the characterized G2/M checkpoints, the tumor cell lines were treated with a range of agents that trigger G2/M arrest. The topoisomerase II inhibitors ICRF193 and etoposide trigger DNA catenation and strand break-sensitive G2/M arrests, respectively (Lock, 1992; Downes *et al.*, 1994), and the microtubule poison nocodazole triggers an anaphase arrest (Sorger *et al.*, 1997). These agents all induced accumulation of cells with 4n DNA and G2/M arrest in all the tumor cell lines (Figure 9). Progression through G2/M in the presence of histone deacetylase inhibitors clearly disrupted normal mitotic processes and led to cell death, indicating that cell cycle progression, particularly through G2/M, was at least partly responsible for the toxic effect of ABHA. Thus imposition of a G2 arrest independently of ABHA should rescue the checkpoint defect in HeLa and MM96L cells. To test this, hydroxyurea-synchronized HeLa cell cultures were treated with ABHA, ICRF193 was added to induce a G2 arrest, and then the cell cycle distribution was assessed at 24 h after release from hydroxyurea. The topoisomerase II inhibitor arrested the cultures in G2 phase and significantly reduced the subdiploid population compared with those treated only with ABHA (31 compared with 60%; $p > 0.01$) to similar levels as ICRF193 treatment alone (Figure 10, A and B). To demonstrate that this rescue was a consequence of the introduction of a G2 phase arrest rather than simply an accumulation of cells with 4n DNA content because of a block in cytokinesis, a similar experiment was performed using nocodazole, which will block cytokinesis. Nocodazole failed to reduce the proportion of the subdiploid cells compared with ABHA alone (Figure 10A).

A High Proportion of Tumor Cell Lines Are Defective for the ABHA-sensitive G2 Checkpoint

A panel of 20 other cell lines have been tested for their cell cycle response and sensitivity to killing by ABHA. These represent immortalized lines, e.g., HaCaT and EBV immortalized lymphoblastoid cell lines (eight lines were tested, but only two representative lines are shown), and a variety of virally transformed and tumor cell lines. Of these, only two lines, MM229 and the Burkitts lymphoma

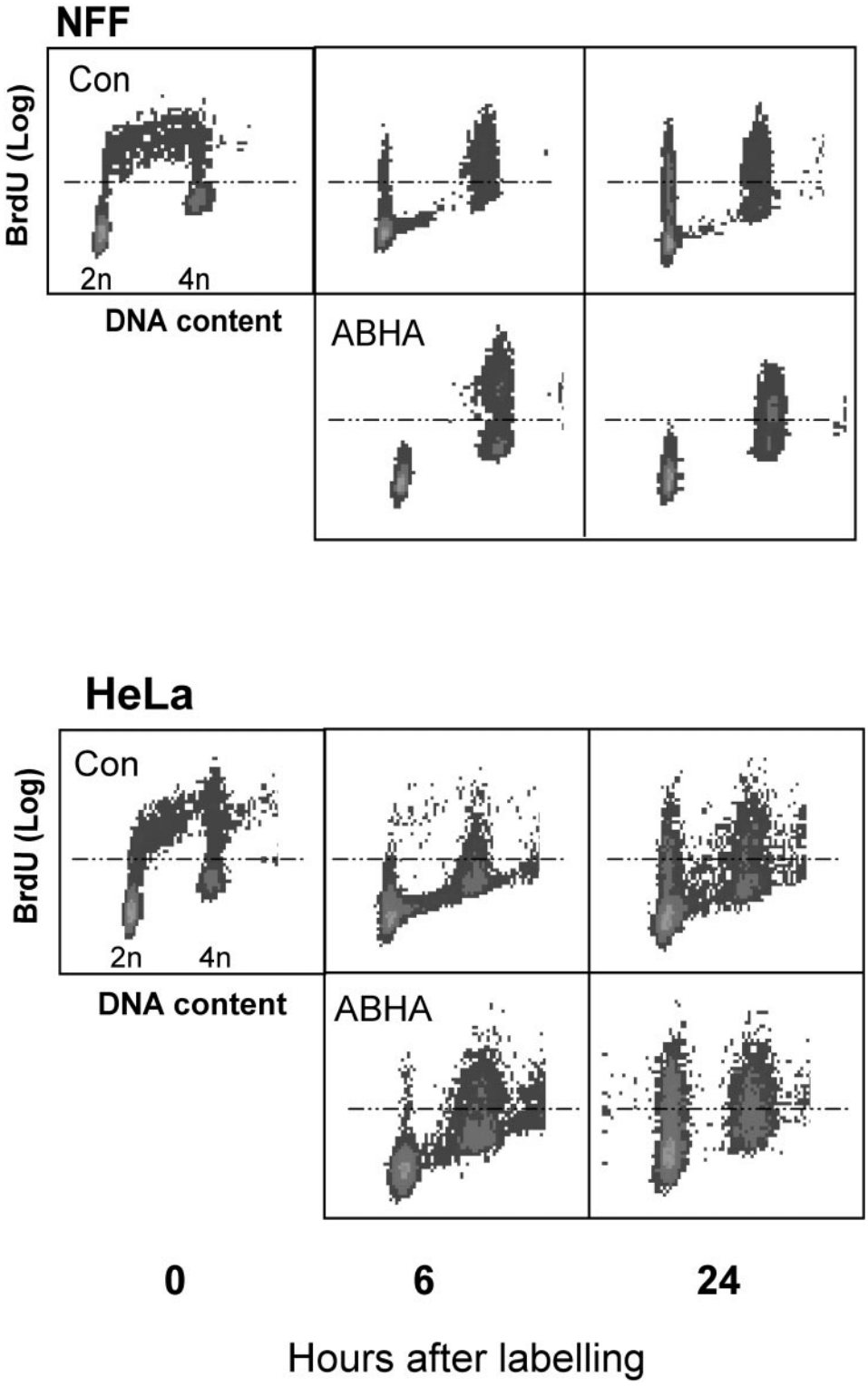

Figure 6. Sensitive but not resistant cells undergo cell division after ABHA treatment. Asynchronous cultures of NFF and HeLa cells were labeled with BrdU for 2 h and then either harvested immediately or 6 and 24 h later, either without or with treatment with 100 μg/ml ABHA. The BrdU-labeled cells (those above the dotted line) pass from S phase (Con, 0 h) into G2/M by 6 h and G1 phase by 24 h (the BrdU-positive cells with 2n DNA content) in the untreated controls and ABHA-treated HeLa cells. No BrdU-labeled G1 phase cells were detected in ABHA-treated NFF cultures at either time.

line DG75, have been found to be resistant to killing by 100 μg/ml ABHA, and both displayed a strong G2/M accumulation at 24 and 48 h after ABHA treatment (Table 1). The remaining cell lines were all sensitive to killing by ABHA, with 60–100% of cells containing <2n DNA by 48 h after treatment. A few of these cell lines showed

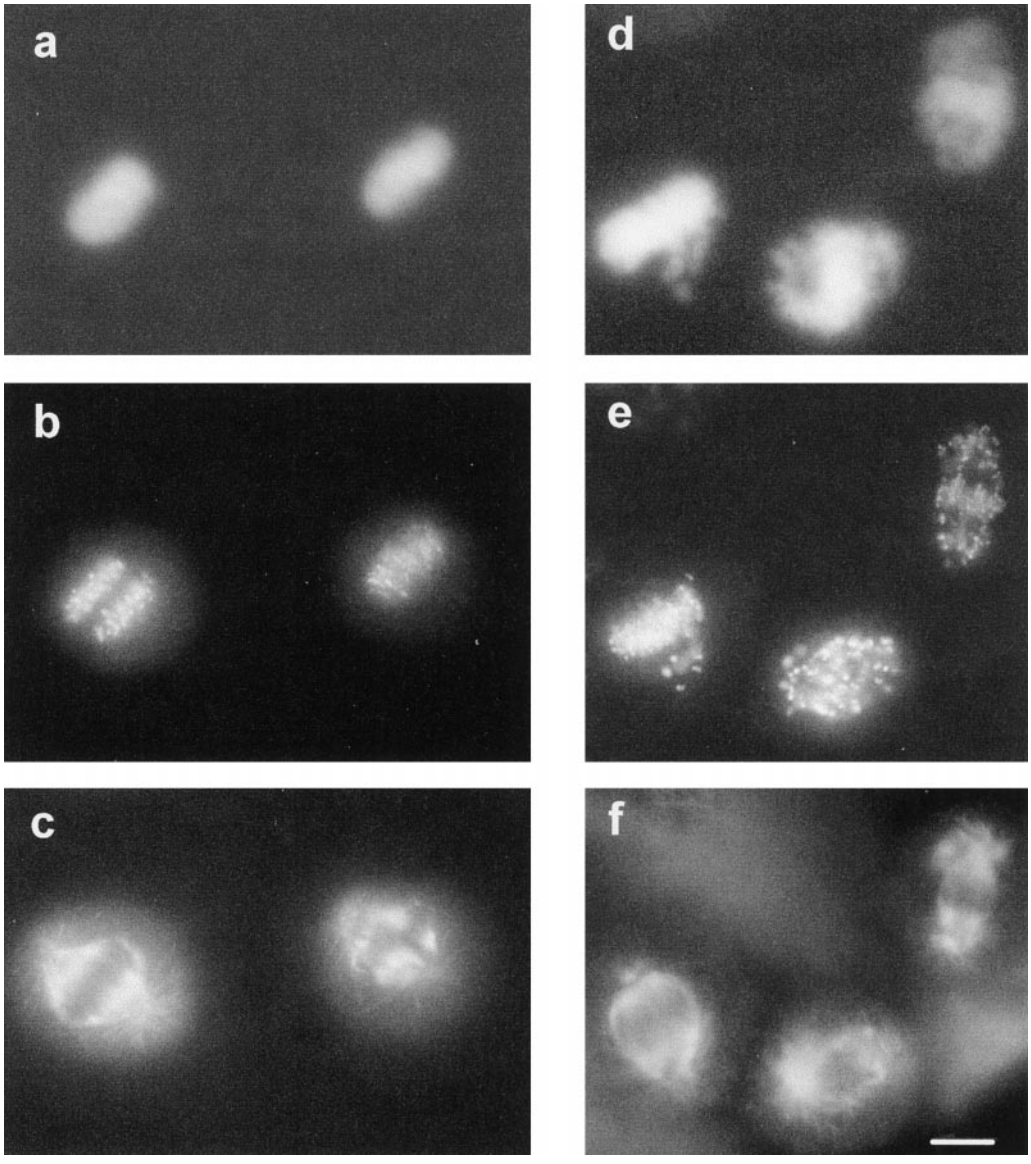

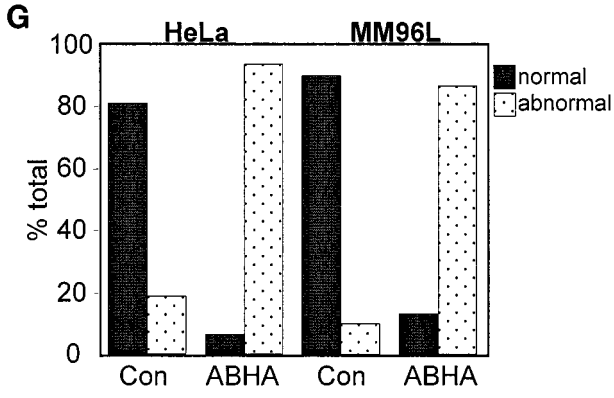

Figure 7. Cells attempting mitosis in the presence of ABHA undergo aberrant mitosis. HeLa cells synchronized by hydroxyurea block and then released and treated without (a–c) or with 100 μg/ml ABHA (d–f), as in Figure 5, were fixed as the cultures entered mitosis. Cells were stained for DNA (a and d), kinetochores (b and e), and microtubules (c and f). The normal congression of condensed chromosomes at metaphase and partitioning at anaphase are clearly observed with the kinetochore staining (a–c). The ABHA-treated mitotic cells contained well-formed spindles, but kinetochore and DNA staining shows chromosomes failing to migrate to the midline of the cell (d–f). Bar, 10 μm. (G) Quantitation of the aberrant mitosis in control and ABHA-treated samples. The numbers of normal and abnormal mitoses were counted for HeLa and MM96L cultures. In each case, between 100 and 200 mitotic figures were counted.

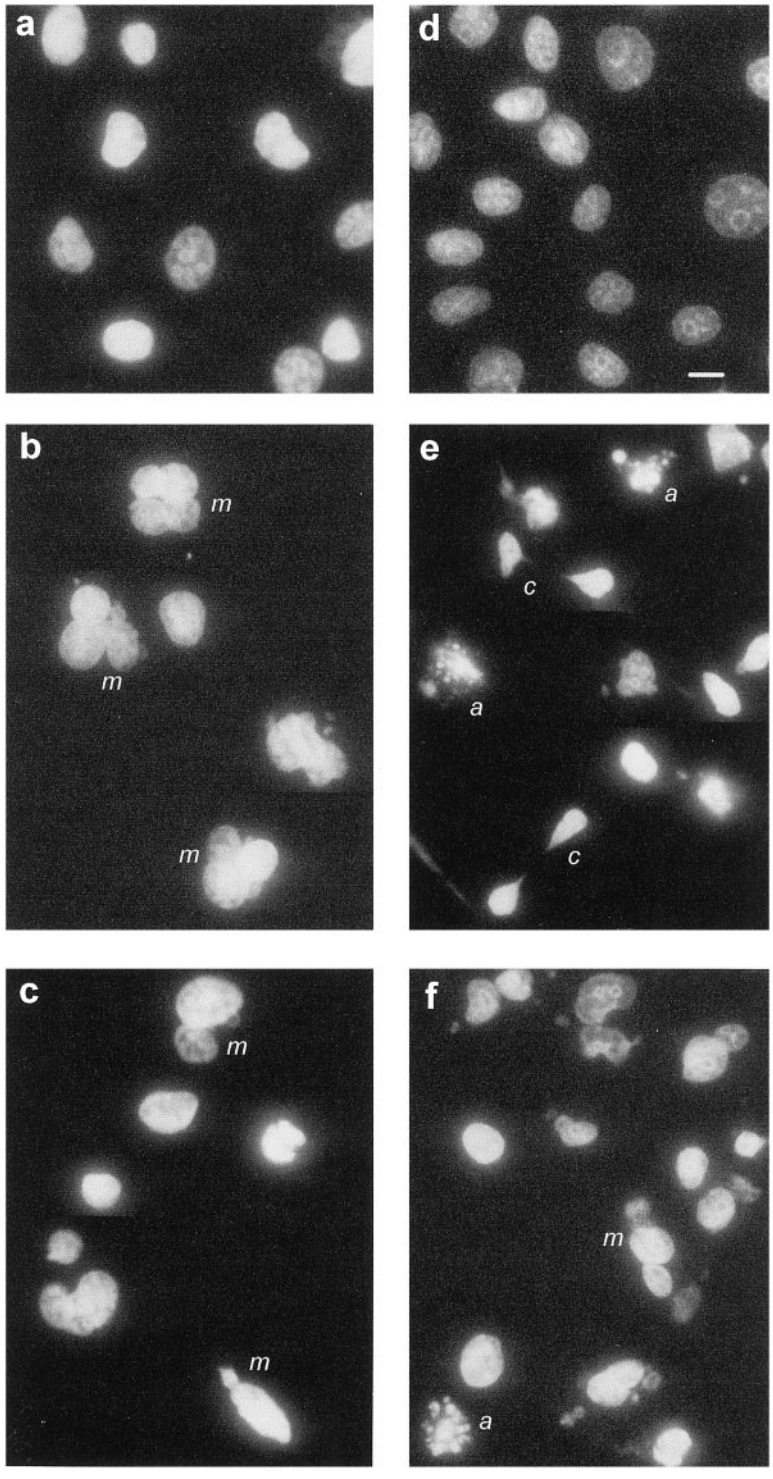

Figure 8. ABHA-induced aberrant mitosis leads to defective cytokinesis and death. MM96L (a–c) and HeLa (d–f) cultures, either control (a and d) or treated for 24 h with 100 μg/ml ABHA (b, c, e, and f) from a hydroxyurea synchrony experiment as in Figure 6, were stained with DAPI for DNA. The presence of multinuclear (*m*), cut phenotype (*c*), and apoptotic cells (*a*) was confirmed by counterstaining for microtubules. Bar, 10 μm.

small increases in the G2/M population at 24 h, e.g., A2058, SVMR, and SCC25, although these were likely to represent multinuclear cells (see Figure 8) and were lost to the subdiploid compartment by 48 h.

DISCUSSION

Histone deacetylase inhibitors have been demonstrated to impose a G1 phase arrest as a result of up-regulated p21

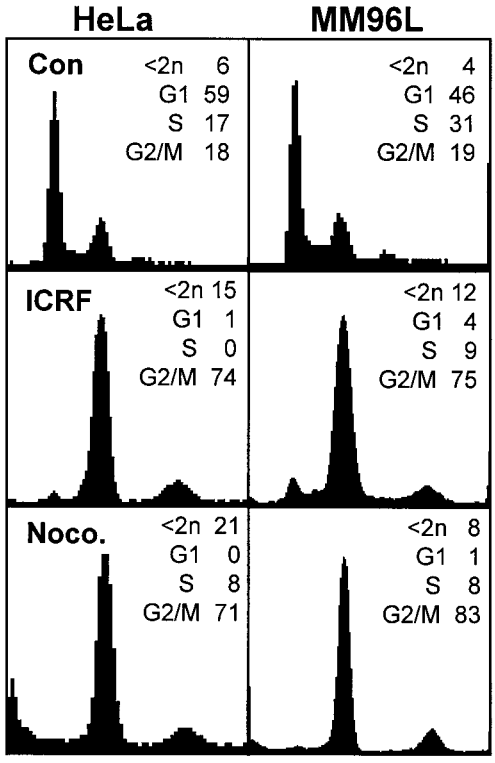

Figure 9. ABHA-sensitive cell lines have functional G2/M checkpoints. Asynchronously growing cultures (Con) or cultures treated with ICRF193 (ICRF) or nocodazole (Noco.) were harvested after 24 h and analyzed by FACS for cell cycle status. In each case, the drugs produced prominent G2/M accumulation with both tumor cell lines. Similar experiments were performed with the topoisomerase II poison etoposide, which produced results similar to those of the topoisomerase II poison ICRF193 (our unpublished results).

expression (Kiyokawa *et al*., 1994; Richon *et al*., 1996; Archer *et al*., 1998; Saito *et al*., 1999). This is also observed in ABHA-treated HeLa and NFF cells, with G1 arrest associated with increased p21 expression and dephosphorylation of Rb and the absence of G1 arrest in MM96L cells, correlated with the absence of p21 expression and maintenance of Rb phosphorylation and cdk2 activity. Down-regulation of cyclin A and cyclin B1 expression observed with ABHA treatment in the resistant NFF cells has also been reported in cells arrested in G2/M after sodium butyrate treatment (Lallemand *et al*., 1999) and appears to be a consequence of prolonged arrest in G2. The down-regulation of cyclins and cdc25C expression in the tumor cell lines is also likely to be a delayed effect, because the synchrony experiments demonstrate that ABHA-treated tumor cells maintain normal expression (our unpublished data) and function of these proteins, indicated by the presence of mitotic cells in the treated cultures. The loss of cyclin and cdc25C expression is likely to reinforce the proliferative arrest.

The data presented in this report support the existence of a G2 checkpoint in ABHA-resistant cells, which is defective in a panel of tumor cell lines. The accumulation of cells with 4n DNA content, the absence of any mitotic figures, and the lack of mitotic cyclin/cdk activity in the synchronized, ABHA-treated NFF cultures are clear evidence of a G2 arrest. The absence of G2 arrest assessed by FACS, apparently normal activation of mitotic cyclin/cdk activities, and high frequency of aberrant mitoses observed in the ABHA-treated tumor cells studied here are good evidence that the ABHA-sensitive cell lines are defective for this protective G2 checkpoint. Reintroduction of a G2 arrest with the topoisomerase II poison ICRF193 had a protective effect, further supporting the notion of a defective checkpoint function in the ABHA-sensitive cells. The ABHA-initiated G2/M checkpoint appears to be different from other known G2 checkpoint mechanisms imposed in response to DNA catentation defects, strand breaks, and spindle defects, because the ABHA-sensitive cell lines examined retained these checkpoint responses but not the histone deacetylase inhibitor-sensitive G2 arrest.

The selective toxicity of ABHA therefore appears to be based on the integrity of the histone deacetylase inhibitor-sensitive G2 checkpoint. For example, the G2 checkpoint was intact in NFF, MM229, and DG75 cells, and these cells were relatively insensitive to the toxic effects of ABHA, with only a small proportion of subdiploid cells by 48 h after treatment. Another group has reported an osteosarcoma cell line that displayed a G2/M arrest after treatment with TSA, and this cell line was also relatively insensitive to killing compared with another tumor cell line that did not G2/M arrest in response to this agent (Sowa *et al*., 1997). The G1 arrest in response to ABHA in a number of ABHA-sensitive tumor cell lines (HeLa, A2058, SK-Mel-13, and HT144) only delayed the appearance of subdiploid cells by 24 h, and these cell lines were >60% subdiploid at 48 h after treatment, compared with cell lines that displayed no cell cycle stage-specific arrest (MM96L, HaCaT, the LCL lines, KJD, SVMR, SCC25, OvCar, and BL30K), which were >50% subdiploid by 24 h after treatment (Table 1).

The loss of the histone deacetylase inhibitor-sensitive checkpoint results in the cells attempting to undergo mitosis in an inappropriate state, leading to noncongression of the condensed chromosomes and ultimately missegregation at cytokinesis. It is surprising that despite the chromosome noncongression observed in the ABHA-treated tumor cells, they do not block in mitosis because of the imposition of an anaphase spindle assembly checkpoint (Sorger *et al*., 1997) but appear to continue through into G1 phase. This phenotype is typical of mutations in BUB1, MAD2, and CENP-E, which are all kinetochore proteins involved in establishing the anaphase checkpoint arrest (Schaar *et al*., 1997; Taylor and McKeon, 1997; Waters *et al*., 1998). The spindle checkpoint function appears to be intact in the cell lines used in this study, because they all block in mitosis when treated with nocodazole, and this may indicate that ABHA affects the expression or function of components of the anaphase checkpoint pathway, e.g., the BUBs and MADs.

The aberrant mitosis is likely to be a trigger for death in the ABHA-treated tumor cells. The ABHA-induced arrest in the resistant cells is in G2 phase, premitotic, before the activation of cyclin A/cdk2 in early G2 phase and cyclin B/cdc2 at G2/M, and this arrest is clearly defective in the ABHA-sensitive cells. Reintroducing a G2 arrest using ICRF193 reduced the level of cell death after ABHA treatment, providing further support for the protective role of

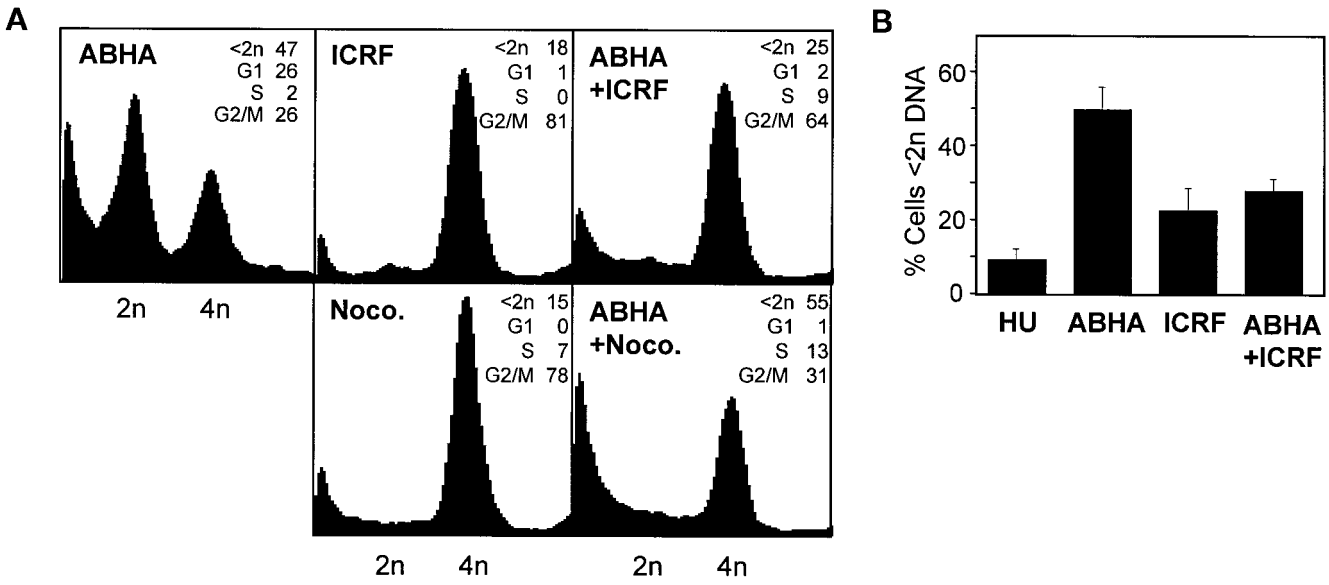

Figure 10. Activation of a G2 checkpoint reduces ABHA-induced cell death. (A) HeLa cells were synchronized by hydroxyurea block release as in Figure 5, treated with ABHA (ABHA), ICRF193 (ICRF), or nocodazole (Noco.), or added in combination as indicated, 2 h after release, and then harvested at 24 h. (B) Proportion of subdiploid cells at 24 h from five independent experiments similar to those in A, with no addition (HU), ABHA only, ICRF193 only, or coaddition of ABHA and ICRF193.

the G2 arrest. However, it is also clear that ABHA disrupts the mitotic spindle checkpoint in the ABHA-sensitive lines. The relationship between the defective G2 arrest and disruption of the later mitotic spindle checkpoint in these cells is unclear, although they may possibly be related. A precedent for a connection between the earlier G2 checkpoint and the later mitotic checkpoint does exist. The caffeine-induced bypass of etoposide-induced G2/M arrest results in disruption of normal chromatid disjunction during mitosis in mammalian cells and catastrophic fracturing of the chromosome by the mitotic spindle during mitosis (Lock *et al.*, 1994). Examination of the mitotic figures in similar caffeine bypass experiments reveals a noncongression phenotype very similar to that observed with ABHA treatment of sensitive cells (our unpublished observations). Thus, it may be that dysfunction of the G2 checkpoint may also disrupt the later mitotic spindle checkpoint, ensuring that cells with significant DNA damage die.

What is the nature of the ABHA-sensitive G2 checkpoint, and how is it inactivated in the tumor cell lines? One possibility is that ABHA alters the expression of a gene or genes involved in G2/M progression, which results in the G2 arrest in resistant cells, and the regulator of this transcriptional program is defective in the ABHA-sensitive cells. An alternative mechanism is a response to the dramatic increase in histone acetylation observed after ABHA treatment of both sensitive and resistant cells (Qiu *et al.*, 1999). This mechanism would prevent cells entering mitosis with hyperacetylated chromatin, which may in turn affect centromere and kinetochore function and thereby disrupt the spindle checkpoint. There may be a defect in either the sensing or signaling mechanism in the tumor cells that results in the loss of the ABHA-sensitive checkpoint arrest. In yeast, TSA has been shown to cause chromosome loss and to disrupt the localization of Swi6p, normally localized to centromeres and involved in normal sister chromatid disjunction (Ekwall *et al.*, 1997). This effect is related to hyperacetylation of centromeric histones and results in missegregation of chromosomes during mitosis. It has also been demonstrated that mutation of the amino-terminal lysine residues normally acetylated in histone H4 results in a G2/M arrest (Megee *et al.*, 1995), and mutations in one of the chromatin remodeling complexes also produces a G2/M arrest and affects the chromatin structure around centromeres (Tsuchiya *et al.*, 1998). Thus in lower eukaryotes a checkpoint mechanism exists that senses the acetylation state of the chromatin and centromere integrity, which consequently may disrupt normal kinetochore function. Considering the high degree of conservation of cell cycle mechanisms from yeast to human, it is likely that the ABHA-sensitive G2 checkpoint we have described here is related to the chromatin acetylation state-sensitive G2/M checkpoint in yeast.

These findings may have clinical relevance in that ABHA represents a novel class of potent chemotherapeutic agents, which selectively kill transformed and tumor cells with defective checkpoint functions. Our initial findings suggest that the ABHA-sensitive cells types may represent a high proportion of epithelial and epidermally derived tumors. The identification of the molecular basis of action of ABHA and its selectivity, especially identification of mutation and deletions of genes that result in the loss of the checkpoint responses in sensitive cells, may

Table 1. G2/M arrest correlates with resistance to killing by ABHA

Cell type	Time (h)	<2n	G1	S	G2/M
MM229 (melanoma)	0	2.6	63.3	18.4	15.7
	24	9.3	20.5	7.9	62.4
	48	33.9	19.6	7.4	39.1
DG75 (Burkitt's lymphoma)	0	1.4	37.0	40.6	20.9
	24	4.2	8.6	32.0	55.1
	48	11.4	20.0	13.2	55.4
HaCaT (immortalized keratinocyte)	0	11.9	41.3	31.4	15.4
	24	69.0	15.8	0	15.0
	48	76.4	13.9	1.3	8.4
LCL-JA (EBV-B cell)	0	2.2	39.1	39.1	13.1
	24	29.3	42.0	6.8	21.9
	48	90.4	7.4	0	2.2
LCL-LO52 (EBV-B cell)	0	28.6	36.5	21.9	13.1
	24	51.3	22.4	0.6	26.3
	48	74.7	19.8	0	4.0
A2058 (melanoma)	0	1.2	51.7	25.9	21.3
	24	11.1	55.1	0.6	33.2
	48	74.8	14.7	0	10.5
MM293 (melanoma)	0	15.7	27.4	35.5	21.5
	24	63.6	25.1	2.5	8.8
	48	76.1	18.8	0	5.1
SK-Mel-13 (melanoma)	0	5.1	60.3	15.3	19.3
	24	20.3	55.3	1.0	23.5
	48	86.3	1.0	4.5	7.7
HT144 (melanoma)	0	2.1	49.1	24.6	24.2
	24	13.4	48.6	7.2	30.9
	48	63.9	22.6	0	13.5
KJD (SV40 keratinocyte)	0	6.9	35.8	28.8	28.5
	24	64.9	17.7	0	17.8
	48	81.4	13.7	0	4.5
SVMR (SV40 keratinocyte)	0	8.8	40.3	32.3	18.6
	24	44.6	20.0	0	35.4
	48	80.1	4.4	0	15.0
SCC25 (squamous cell carcinoma)	0	23.2	31.6	22.2	23.0
	24	53.2	11.8	1.4	33.6
	48	77.3	1.4	0	21.4
OvCar (ovarian cancer)	0	25.4	24.8	28.5	21.3
	24	100	0	0	0
	48	100	0	0	0
BL30 (Burkitt's lymphoma)	0	8.4	36.0	31.6	24.1
	24	65.4	17.8	4.1	12.6
	48	74.8	18.7	6.5	0

Asynchronously growing cultures of each cell line were treated without (time 0) or with 100 μg/ml ABHA for 24 and 48 h and then harvested, and the cell cycle status was assessed by FACS. The percentage of cells in each cell cycle phase, and the subdiploid cell, are shown. These data are representative of two to four independent experiments.

lead to more effective treatment of tumors by more directly targeting the checkpoint.

ACKNOWLEDGMENTS

We thank Dr. J.B. Rattner for the gift of the human kinetochore antiserum, Dr. A.M Creighton for the ICRF193, Dr. Nick Saunders (University of Queensland) for the SCC cell line, and Drs. Sherilyn Goldstone and Sandra Pavey for critical reading of the manuscript. This work was supported by grants from the National Health and Medical Research Council of Australia and the Queensland Cancer Fund. B.G.G. is an Australian Research Fellow.

REFERENCES

Archer, S.Y., Meng, S., Shei, A., and Hodin, R.A. (1998). p21(WAF1) is required for butyrate-mediated growth inhibition of human colon cancer cells. Proc. Natl. Acad. Sci. USA *95*, 6791–6796.

Breslow, R., Jursic, B., Yan, Z.F., Friedman, E., Leng, L., Ngo, L., Rifkind, R.A., and Marks, P.A. (1991). Potent cytodifferentiating agents related to hexamethylenebisacetamide. Proc. Natl. Acad. Sci. USA *88*, 5542–5546.

Darzynkiewicz, Z., Bruno, S., Del Bino, G., Gorczyca, W., Hotz, M.A., Lassota, P., and Traganos, F. (1992). Features of apoptotic cells measured by flow cytometry. Cytometry *13*, 795–808.

Downes, C.S., Clarke, D.J., Mullinger, A.M., Gimenez-Abian, J.F., Creighton, A.M., and Johnson, R.T. (1994). A topoisomerase II-dependent G2 cycle checkpoint in mammalian cells. Nature *372*, 467–470.

Dulic, V., Kaufmann, W.K., Wilson, S.J., Tlsty, T.D., Lees, E., Harper, J.W., Elledge, S.J., and Reed, S.I. (1994). p53-dependent inhibition of cyclin-dependent kinase activities in human fibroblasts during radiation-induced G1 arrest. Cell *76*, 1013–1023.

Dulic, V., Lees, E., and Reed, S.I. (1992). Association of human cyclin E with a periodic G1-S phase protein kinase. Science *257*, 1958–1961.

Ekwall, K., Olsson, T., Turner, B.M., Cranston, G., and Allshire, R.C. (1997). Transient inhibition of histone deacetylation alters the structural and functional imprint at fission yeast centromeres. Cell *91*, 1021–1032.

Elledge, S.J. (1996). Cell cycle checkpoints: preventing an identity crisis. Science *274*, 1664–1672.

Gabrielli, B.G., Clark, J.M., McCormack, A.K., and Ellem, K.A. (1997). Ultraviolet light-induced G2 phase cell cycle checkpoint blocks cdc25-dependent progression into mitosis. Oncogene *15*, 749–758.

Gabrielli, B.G., De Souza, C.P., Tonks, I.D., Clark, J.M., Hayward, N.K., and Ellem, K.A. (1996). Cytoplasmic accumulation of cdc25B phosphatase in mitosis triggers centrosomal microtubule nucleation in HeLa cells. J. Cell Sci. *109*, 1081–1093.

Grunstein, M. (1997). Histone acetylation in chromatin structure and transcription. Nature *389*, 349–352.

Hartwell, L.H., and Kastan, M.B. (1994). Cell cycle control and cancer. Science *266*, 1821–1828.

Jin, P., Gu, Y., and Morgan, D.O. (1996). Role of inhibitory CDC2 phosphorylation in radiation-induced G2 arrest in human cells. J. Cell Biol. *134*, 963–970.

Kiyokawa, H., Richon, V.M., Rifkind, R.A., and Marks, P.A. (1994). Suppression of cyclin-dependent kinase 4 during induced differentiation of erythroleukemia cells. Mol. Cell. Biol. *14*, 7195–7203.

Lallemand, F., Courilleau, D., Buquet-Fagot, C., Atfi, A., Montagne, M.N., and Mester, J. (1999). Sodium butyrate induces G2 arrest in the human breast cancer cells MDA-MB-231 and renders them competent for DNA rereplication. Exp. Cell Res. *247*, 432–440.

Lavin, M.F., and Shiloh, Y. (1996). Ataxia-telangiectasia: a multifaceted genetic disorder associated with defective signal transduction. Curr. Opin. Immunol. *8*, 459–464.

Lengauer, C., Kinzler, K.W., and Vogelstein, B. (1997). Genetic instability in colorectal cancers. Nature *386*, 623–627.

Lock, R.B. (1992). Inhibition of p34cdc2 kinase activation, p34cdc2 tyrosine dephosphorylation, and mitotic progression in Chinese hamster ovary cells exposed to etoposide. Cancer Res. *52*, 1817–1822.

Lock, R.B., Galperina, O.V., Feldhoff, R.C., and Rhodes, L.J. (1994). Concentration-dependent differences in the mechanisms by which

caffeine potentiates etoposide cytotoxicity in HeLa cells. Cancer Res. *54*, 4933–4939.

Megee, P.C., Morgan, B.A., and Smith, M.M. (1995). Histone H4 and the maintenance of genome integrity. Genes Dev. *9*, 1716–1727.

Morgan, D.O. (1995). Principles of CDK regulation. Nature *374*, 131–134.

Pagano, M., Pepperkok, R., Lukas, J., Baldin, V., Ansorge, W., Bartek, J., and Draetta, G. (1993). Regulation of the cell cycle by the cdk2 protein kinase in cultured human fibroblasts. J. Cell Biol. *121*, 101–111.

Parsons, P.G., Hansen, C., Fairlie, D.P., West, M.L., Danoy, P.A., Sturm, R.A., Dunn, L.S., Pedley, J., and Ablett, E.M. (1997). Tumor selectivity and transcriptional activation by azelaic bishydroxamic acid in human melanocytic cells. Biochem. Pharmacol. *53*, 1719–1724.

Qiu, L., Kelso, M.J., Hansen, C., West, M.L., Fairlie, D.P., and Parsons, P.G. (1999). Anti-tumor activity in vitro and in vivo of selective differentiating agents containing hydroxamate. Br. J. Cancer *80*, 1252–1258.

Rhind, N., Furnari, B., and Russell, P. (1997). Cdc2 tyrosine phosphorylation is required for the DNA damage checkpoint in fission yeast. Genes Dev. *11*, 504–511.

Richon, V.M., Emiliani, S., Verdin, E., Webb, Y., Breslow, R., Rifkind, R.A., and Marks, P.A. (1998). A class of hybrid polar inducers of transformed cell differentiation inhibits histone deacetylases. Proc. Natl. Acad. Sci. USA *95*, 3003–3007.

Richon, V.M., Webb, Y., Merger, R., Sheppard, T., Jursic, B., Ngo, L., Civoli, F., Breslow, R., Rifkind, R.A., and Marks, P.A. (1996). Second generation hybrid polar compounds are potent inducers of transformed cell differentiation. Proc. Natl. Acad. Sci. USA *93*, 5705–5708.

Rosenblatt, J., Gu, Y., and Morgan, D.O. (1992). Human cyclin-dependent kinase 2 is activated during the S and G2 phases of the cell cycle and associates with cyclin A. Proc. Natl. Acad. Sci. USA *89*, 2824–2828.

Saito, A., Yamashita, T., Mariko, Y., Nosaka, Y., Tsuchiya, K., Ando, T., Suzuki, T., Tsuruo, T., and Nakanishi, O. (1999). A synthetic inhibitor of histone deacetylase, MS-27-275, with marked in vivo antitumor activity against human tumors. Proc. Natl. Acad. Sci. USA *96*, 4592–4597.

Saunders, N., Dicker, A., Popa, C., Jones, S., and Dahler, A. (1999). Histone deacetylase inhibitors as potential anti-skin cancer agents. Cancer Res. *59*, 399–404.

Schaar, B.T., Chan, G.K., Maddox, P., Salmon, E.D., and Yen, T.J. (1997). CENP-E function at kinetochores is essential for chromosome alignment. J. Cell Biol. *139*, 1373–1382.

Sherr, C.J. (1996). Cancer cell cycles. Science *274*, 1672–1677.

Sherr, C.J., and Roberts, J.M. (1995). Inhibitors of mammalian G1 cyclin-dependent kinases. Genes Dev. *9*, 1149–1163.

Sorger, P.K., Dobles, M., Tournebize, R., and Hyman, A.A. (1997). Coupling cell division and cell death to microtubule dynamics. Curr. Opin. Cell Biol. *9*, 807–814.

Sowa, Y., Orita, T., Minamikawa, S., Nakano, K., Mizuno, T., Nomura, H., and Sakai, T. (1997). Histone deacetylase inhibitor activates the WAF1/Cip1 gene promoter through the Sp1 sites. Biochem. Biophys. Res. Commun. *241*, 142–150.

Taylor, S.S., and McKeon, F. (1997). Kinetochore localization of murine Bub1 is required for normal mitotic timing and checkpoint response to spindle damage. Cell *89*, 727–735.

Tsuchiya, E., Hosotani, T., and Miyakawa, T. (1998). A mutation in NPS1/STH1, an essential gene encoding a component of a novel chromatin-remodeling complex RSC, alters the chromatin structure of *Saccharomyces cerevisiae* centromeres. Nucleic Acids Res. *26*, 3286–3292.

Wang, J.Y. (1998). Cellular responses to DNA damage. Curr. Opin. Cell Biol. *10*, 240–247.

Waters, J.C., Chen, R.H., Murray, A.W., and Salmon, E.D. (1998). Localization of Mad2 to kinetochores depends on microtubule attachment, not tension. J. Cell Biol. *141*, 1181–1191.